

N90-28750

3-D Vision System Integrated Dexterous Hand

Ren C. Luo and Youn-Sik Han

Robotics and Intelligent Systems Laboratory
Department of Electrical and Computer Engineering
North Carolina State University
Raleigh, NC 27695-7911

1. Introduction

The limited capabilities of conventional two-jaw type grippers have prompted research efforts concentrated on the development of a multifingered hand which can grasp an object of arbitrary shape and manipulate it within its grasp.

Most multifingered hands use a tendon mechanism to minimize the size and weight of the hand. Such tendon mechanisms suffer from the problems of stiction and friction of the tendons. This results in a reduction of control accuracy. In order to overcome these problems in control accuracy and to give the hand more flexibility and intelligence, a design for a 3-D vision system integrated dexterous hand using motor control is presented.

The proposed hand is composed of three three-jointed grasping fingers with tactile sensors on their tips, a two-jointed 'eyed finger' with a microcamera in its distal part, and another two-jointed 'laser-emitting finger' with a cross-shaped laser beam emitting diode in its distal part. The two non-grasping fingers allow 3-D vision capability and can rotate around the hand to see and measure the sides of grasped objects and in its task environment.

Little research effort has been focused on the application of 3-D vision-in-hand systems to perform the task of grasping and manipulating an object. In this paper, an algorithm which determines the range and local orientation of the contact surface using a cross-shaped laser light beam is introduced together with some potential applications.

Grasping and manipulating an object with a multifingered hand is a complicated task and there still remain a number of unsolved problems. One inherent and important problem is the determination of the proper internal grasping forces. Some work has been concentrated on grasping or manipulation force analysis, however, finger force determination has not been addressed. This problem can be solved efficiently using the geometric information of the objects to be grasped acquired by the 3-D vision-in-hand system. In this paper, an efficient method for the finger force calculation is presented which uses the measured contact surface normals of an object.

Current industrial manipulators are usually equipped with two-jaw grippers. These grippers not only have difficulty in handling objects with an arbitrarily complex geometry, but also have difficulty in manipulating objects within their grippers.

An alternative solution to this problem is to design and build a flexible gripping device which is capable of a large variety of tasks. Several investigators have developed designs for such devices. A number of multi-fingered multi-jointed hands have been developed, ranging from the nine degree of freedom (DOF) Stanford/JPL hand to the 16

DOF Utah/MIT hand. Most of these multi-fingered hands are driven through a cable transmission to minimize the size and weight of the hand and to give compliance to the finger at the expense of problems such as stiction and friction, control stability, time response, and accuracy. To compensate for the adverse effects of a cable transmission mechanism, it is necessary to develop relatively complex low-level control systems that include cable tension control. These hand and finger configurations tend to mimic the human hand, which is not necessarily the best configuration for a mechanical hand.

In this paper, we have developed a more compact design for a dexterous hand to overcome the difficulties resulting from the use of a cable transmission. Furthermore, we are currently developing a hand-based 3-D laser range finder which can rotate around the hand so that it can perceive the object being grasped.

2. Hand Design

Recently, as a result of an increased research effort in the field of multifingered hands, several hands have been developed. Almost all of the multifingered hands developed are human-like, but this does not seem to be the optimal solution to the problem of grasping objects of various shape and manipulating them for various tasks--even though human-like hands have some advantages when imitating the function of human hand, especially in a teleoperation system.

Most of the multifingered hands that have been developed have a relatively small hand workspace [Kerr et al 86] due to their human-like fingers and the finger joint arrangement. The first and middle fingers are placed near to each other, limiting the space to cooperate with each other. In addition, the first joint of each finger is a yawing joint, not a twisting joint. If we allow some distance between fingers and make the first joint of each finger a twisting joint, then the hand workspace will be enlarged and have more dexterity.

Furthermore, most of these multifingered hands have adopted a cable transmission system and their actuators are located remotely. This makes the design of the control system very difficult because of the deflection, friction, and stiction of the cables. Thus it is hard to control the fingertip position and force precisely during manipulation. Therefore, it is better to design the transmission system so that it is rigid and has a shorter transmission length by placing the motors near to the fingers.

For the reasons given above, we have developed a new design for a five-fingered hand where one of the fingers is eyed and one emits a laser beam. The remaining three fingers are used for grasping. The nongrasping fingers can rotate around the hand as shown in the illustrative scheme (see Fig.1).

It is necessary for a hand to have a minimum of three fingers in order to grasp an object of arbitrary shape. Thus, the proposed hand has three grasping fingers. In order to position the fingertip everywhere within the workspace, it is necessary for each finger to have minimum of three degrees of freedom. Thus, each finger has been designed for having three joints. The kinematic arrangement of finger joints are unlike the human hand. Three fingers are equally spaced. The first joint of all three grasping fingers is a revolving joint which can provide a larger hand workspace and more dexterity.

Each of the nongrasping fingers is composed of two joints so that it can possibly reorient itself in the direction of the object to be grasped in the adjacent task environment. A micro-camera is located in the distal part of eyed finger and a laser diode is implanted in the laser beam emitting finger.

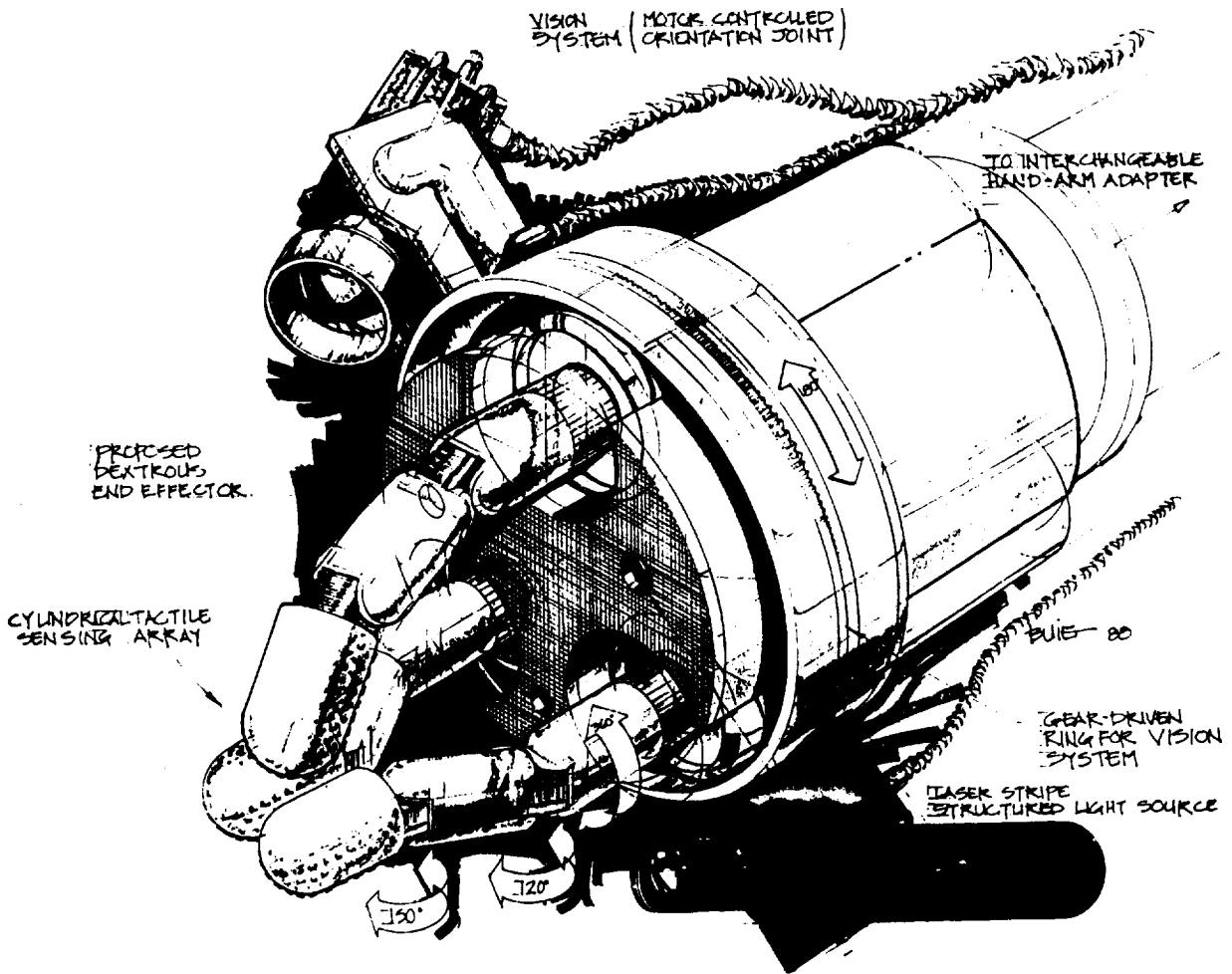


Figure 1. Proposed illustrative scheme for a 3-D vision integrated dexterous hand

Each joint is driven by a micro dc servomotor with a reduction gearhead through the gear and/or chain transmission. This provides for more rigidity in the control system as compared to the remote cable transmission.

3. Grasping Algorithm using 3-D Visual Data

Manipulating an object with a multifingered hand is a non-trivial task. Not only are the kinematic relationships between the finger joint motions and the object motion complicated, but during the execution of the task the hand must also firmly grasp the object and exert some force and moments to the task environment.

Salisbury has investigated grasping or manipulation force stability [Salisbury 82]. Since the object is overconstrained by the multifinger contacts, the system is statically indeterminate. Several other researchers have determined the optimal internal forces. Kerr has determined that the optimal internal forces are those with minimum norm under an approximated frictional constraints [Kerr 86]. Hollerbach has developed a fast

algorithm to calculate the fingertip forces without using the Jacobian for the given external and internal forces [Hollerbach et al 86]. Yoshikawa defined the concept of internal forces as grasping forces [Yoshikawa et al 87]. Here we develop an approach to determine the internal grasping forces and finger forces based on the contact surface information that can be measured by the proposed 3-D laser range finding devices.

3.1 Determination of the Internal Grasping Force

Each fingertip force, f_i , can be decomposed into two components: the internal grasping force, f_{gi} , and the manipulating forces, f_{mi} , where subscript i denotes the finger ($i = 1,2,3$). The internal grasping force components are defined as these forces that contribute to the grasping of a massless rigid object, and the manipulating force components are defined as those forces that contribute to generate the resultant net forces used to move an object. The main feature of the internal grasping forces is that the forces are equilibrating by themselves and thus do not have any effect on the resultant forces and moments. If we can determine these internal grasping forces, then the manipulating forces and each fingertip force can easily be determined.

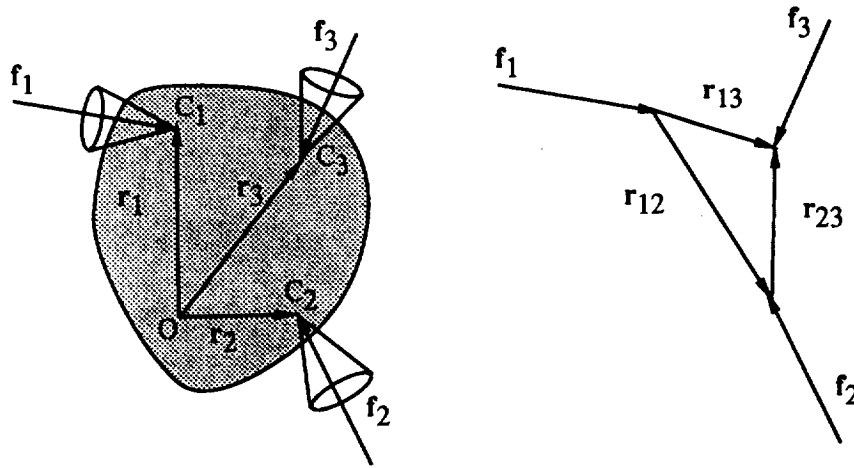


Figure 2. Illustration of three points contact with friction on an object

There are an infinite number of solutions for the internal grasping forces because the system is statically indeterminate. This arbitrariness has three degrees of freedom when we use a hard finger (friction point contact) model in three finger grasping. However, by considering the friction coefficient between the contact points and the contact surface, we can reduce the arbitrariness of the solutions to the degree of one. Also, considering each total fingertip force as being limited by the maximum exorable finger joint driving torque, we can finally determine the internal grasping forces. Since the internal grasping force components of the fingertip forces (the f_{gi} 's) are equilibrating by themselves and do not contribute to the resultant force, we can formulate the equations as follows.

$$\begin{aligned} f_{g1} + f_{g2} + f_{g3} &= 0 \\ f_{g1} \cdot r_1 + f_{g2} \cdot r_2 + f_{g3} \cdot r_3 &= 0 \end{aligned} \quad (1)$$

where

r_i : position vector of the i th contact point

This means that the f_{gi} 's form a closed triangle on the grasping plane, where the contact points (the C_i 's) lie on the plane and the lines through the C_i 's are intersecting at one point, G (see Figure 3). Let G be called the grasp center point.

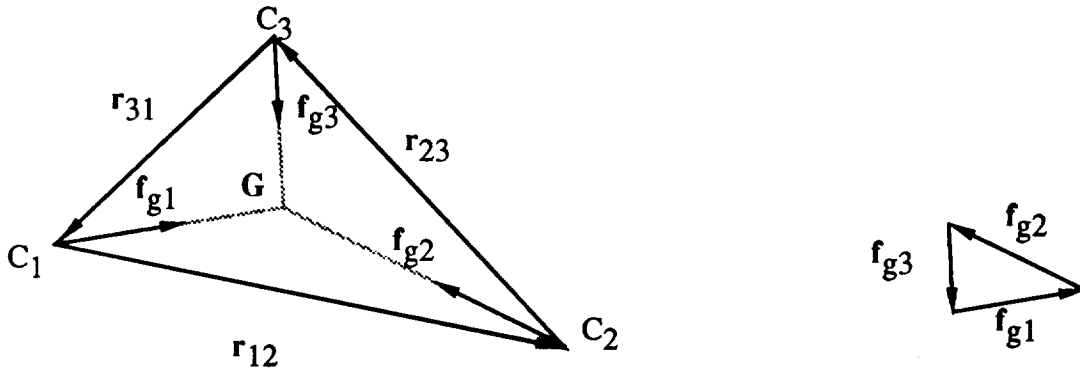


Figure 3. Internal grasping forces and grasp centerpoint

The grasp center point should be inside the common intersection volume of the three friction cones whose center axes are contacting the surface normal vectors, a_i . Also, G should lie on the grasping plane (see Figure 4).

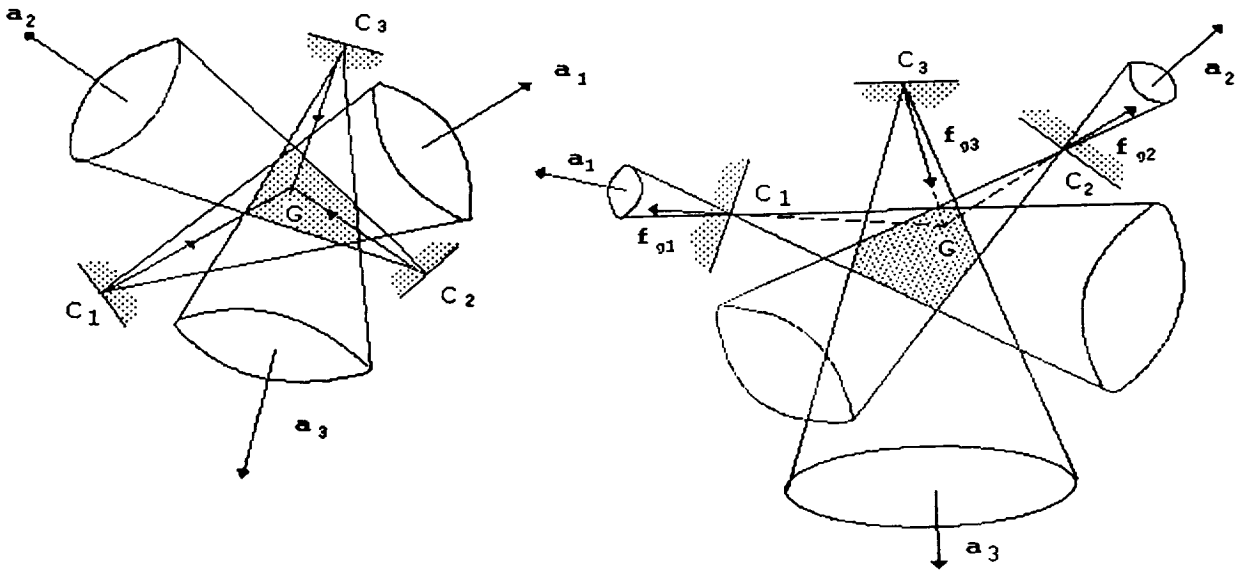


Figure 4. Friction cones and contact normal vectors

Therefore, if we can properly choose the grasp center point, G , for given contact surface normal vectors a_i , we can reduce the three degrees of arbitrariness to one by using the equilibrium equations of the internal grasping forces (see Figure 5).

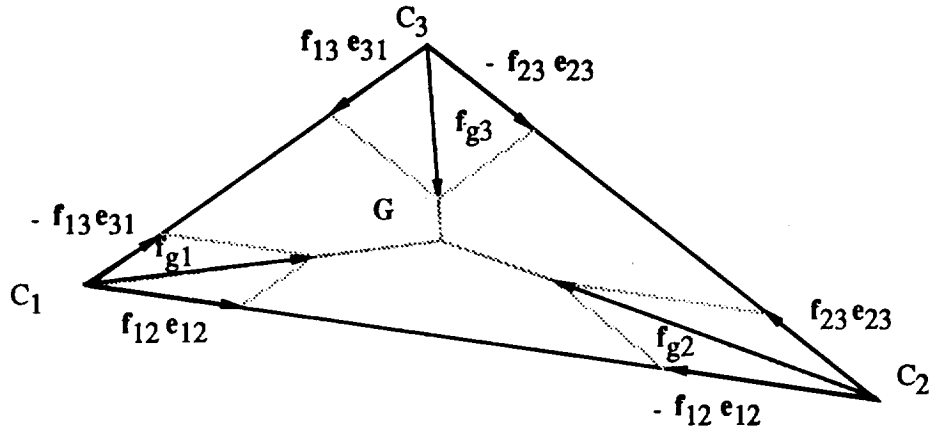


Fig 5. Decomposition of internal grasping force components

Let \mathbf{a}_i^* be the projection of the contact surface normal vector \mathbf{a}_i onto the grasp plane. Then, in general, the prolonged lines of the \mathbf{a}_i^* form a triangle on the grasp plane. We can determine the grasp center point G to be the center point of the inward tangent circle of this triangle so that the sum of deviations from each line will be minimized (see Figure 6).

Then, the internal grasping forces \mathbf{f}_{gi} act along the unit vector

$$\mathbf{e}_{iG} = (\mathbf{r}_G - \mathbf{r}_i) / \|\mathbf{r}_G - \mathbf{r}_i\| \quad (2)$$

where \mathbf{r}_G is the position vector of the grasp center point G .

Since the internal grasping forces are located inside of the friction cones, the constraints of equation (3)

$$|\mathbf{a}_i \cdot \mathbf{e}_{iG}| \leq \cos(\tan^{-1} u_i) \quad (3)$$

should be satisfied. (Here u_i is the friction coefficient of each finger.) Otherwise, the object cannot be grasped with these contacts.

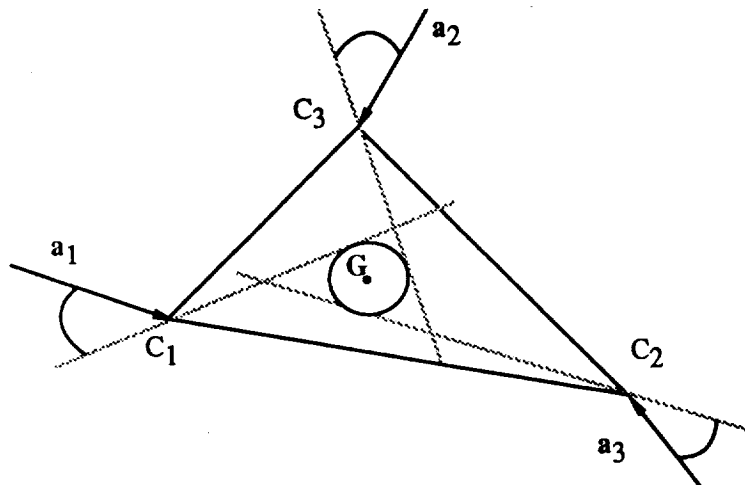


Figure 6. Determination of the grasp center point G

Once we have determined the grasp center point G, we can easily determine the internal grasping force components from the equilibrium equations.

The internal grasping force \mathbf{f}_{gi} can be decomposed into two components which are parallel to the edges of the grasp triangle. Let

$$\begin{aligned} \mathbf{e}_{ij} &= \mathbf{r}_{ij} / \|\mathbf{r}_{ij}\| \\ \mathbf{r}_{ij} &= \mathbf{r}_j - \mathbf{r}_i \end{aligned}$$

Then,

$$\begin{aligned} \mathbf{f}_{g1} &= (\mathbf{f}_{g1} \cdot \mathbf{e}_{31}) \mathbf{e}_{31} + (\mathbf{f}_{g1} \cdot \mathbf{e}_{12}) \mathbf{e}_{12} \\ \mathbf{f}_{g2} &= (\mathbf{f}_{g2} \cdot \mathbf{e}_{12}) \mathbf{e}_{12} + (\mathbf{f}_{g2} \cdot \mathbf{e}_{23}) \mathbf{e}_{23} \\ \mathbf{f}_{g3} &= (\mathbf{f}_{g3} \cdot \mathbf{e}_{23}) \mathbf{e}_{23} + (\mathbf{f}_{g3} \cdot \mathbf{e}_{31}) \mathbf{e}_{31} \end{aligned} \quad (4)$$

3.2 Determination of Fingertip Force \mathbf{f}_i

As mentioned in previous section, we can determine the internal grasping force \mathbf{f}_{gi} and its component magnitude \mathbf{f}_{ij} . The relationship between the fingertip forces, \mathbf{f}_i , and the internal grasping force components can be expressed as

$$\mathbf{f}_{ij} = (\mathbf{f}_i \cdot \mathbf{e}_{ij} - \mathbf{f}_j \cdot \mathbf{e}_{ij}) \mathbf{e}_{ij}$$

This means that the internal grasping force component magnitude \mathbf{f}_{ij} is the difference in the projections of the fingertip forces \mathbf{f}_i and \mathbf{f}_j to the intercontact line \mathbf{r}_{ij} . The above relationship can be rewritten as

$$(\mathbf{f}_i - \mathbf{f}_j) \cdot \mathbf{r}_{ij} = \mathbf{f}_{ij} \cdot \|\mathbf{r}_{ij}\|$$

Then, by applying Hollerbach's method [Hollerbach et al 86], we can determine the fingertip forces (the \mathbf{f}_i s). These fingertip forces also should lie inside of the friction cone

$$\mathbf{f}_i / \|\mathbf{f}_i\| \cdot \mathbf{a}_i \leq \cos(\tan^{-1} u_i)$$

where u_i is the friction coefficient between the fingertip and the contact surface. If the fingertip force does not meet this criterion, it can not be applied by the hard finger contact, and thus we should find another place to locate the fingertip.

3.3 Determination of Finger Joint Torques

Taking advantage of the kinematic features of the fingers of the proposed hand, each joint torque t_{ik} can easily be expressed as a function of the grasp intensity g from the fingertip force \mathbf{f}_i , where subscript k denotes each finger joint number. Since t_{ik} should not exceed the limit of maximum torque t_{ikmax} , we can determine the value of grasp intensity g .

Since the internal grasping force does not contribute to the resultant force and moment, adjusting the value of grasp intensity (or grasp security) g can result in more flexibility in the control of the fingertip forces.

4. 3-D Vision Integrated with the Hand for Grasp planning and Manipulation

As previously mentioned in the determination of finger force, the role of 3-D vision in giving information about contact locations (contact point vectors r_i and contact surface normal vectors a_i) is very important in the grasping planning stage. Also, 3-D vision can play a major role during the reorientation of a grasped object during task execution.

The proposed 3-D vision system is composed of one small camera and one cross-shaped laser beam emitter, each of which is mounted on the distal part of two separate fingers. One finger is called the eyed finger and the other is called the laser beam emitting finger. Each of these two fingers has one bending joint and is mounted on rotating gears around the hand. Thus the camera will be able to see any side of the grasped object, and can measure the distance to any point on surface of the object to be grasped and the surface orientation of the object.

After grasping an object, the status of the grasped object may not be the same as expected because of measurement and control error. Since the main control scheme of the multifingered hand is force control, object motion is subject to the interaction between the fingertip forces. Furthermore, there are many uncertainties in the contact mechanics and the grasped object may not be the expected state. With the proposed 3-D vision system, we can measure the status of the grasped object, namely, its orientation and the position of a particular part of the object with respect to the hand frame. Figure 7 illustrates this basic concept.

We have simulated the operation of this sensor based dexterous hand using an Appollo graphics workstation. Figure 8 shows an example of the simulation.

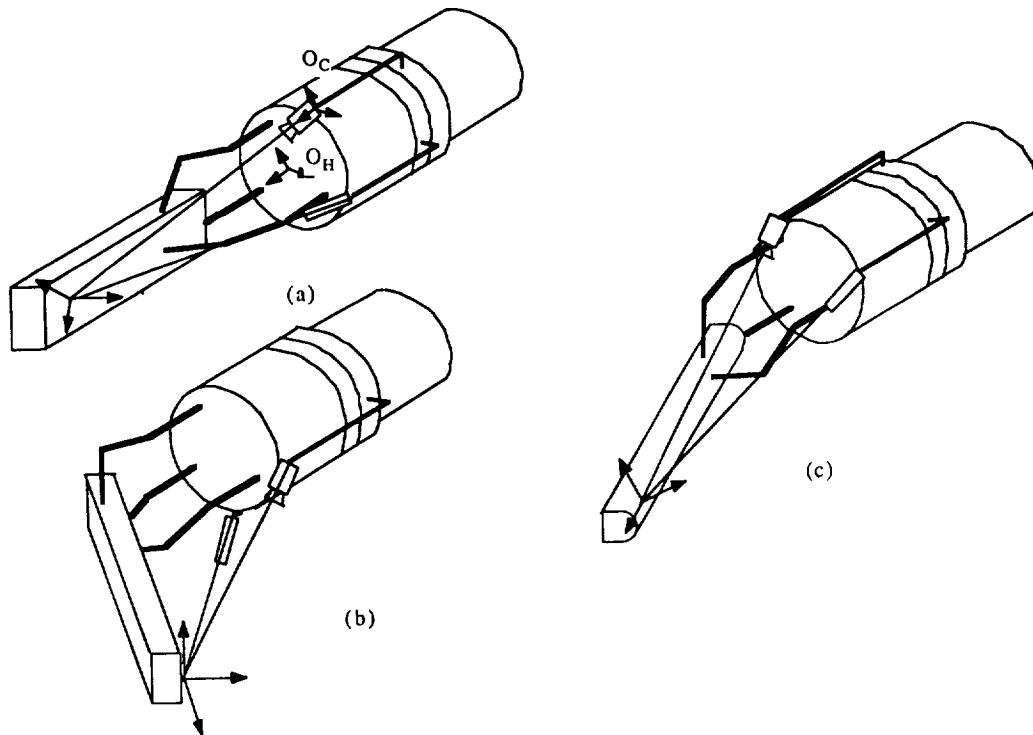


Figure 7. Object posture measurements

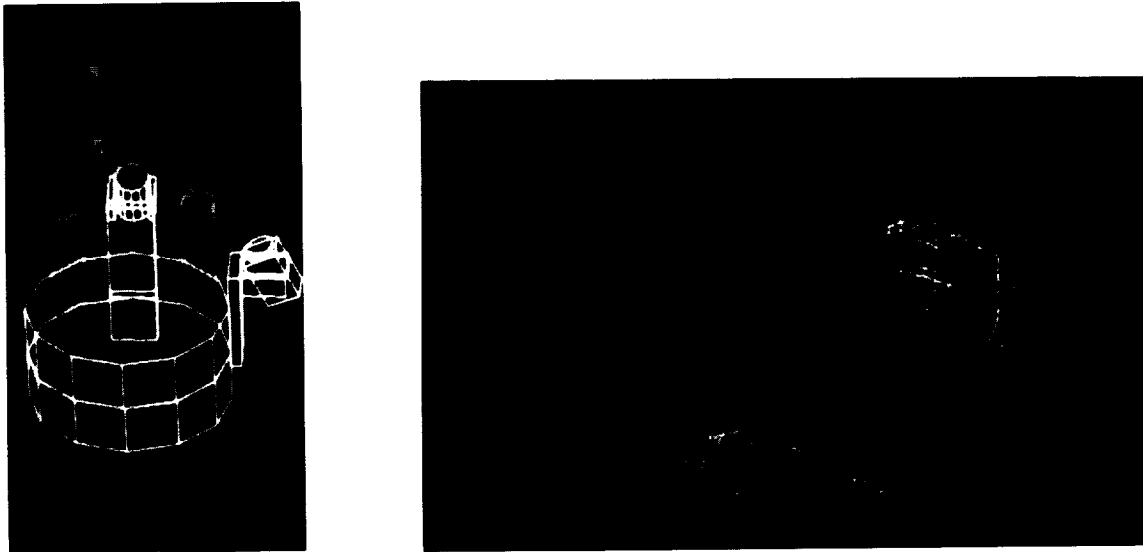


Figure 8. Two views of simulated design of sensor based dexterous hand

REFERENCES

- Biggers, K.B., Jacobsen, S.C., Gerpheide, G.E. (1986). Low Level Control of the Utah/MIT Hand. 1986 IEEE International Conference on Robotics and Automation, pp. 61-66.
- Hollerbach, J.M., Narashman, S., Wood, J.E. (1986). Finger Force Computation without Grip Jacobian, 1986 IEEE International Conference on Robotics and Automation, pp. 871-875.
- Jacobsen, S.C., Iversen, E.K., Biggers, K.B., Knutti, D.F., Johnson, R.T. (1986). Design of the Utah/MIT Dexterous Hand. 1986 IEEE International Conference on Robotics and Automation, pp.1520-1532.
- Jameson, J.W., Leifer, L.J. (1986). Quasi-static Analysis : A Method for Predicting Grasp Stability. 1986 IEEE International Conference on Robotics and Automation, pp. 876-883.
- Kerr, J., Roth, B., (1986). Analysis of Multifingered Hand. International Journal of Robotics Research, vol. 4, no. 4, pp. 3-17.
- Narashiman, S., Siegel, D.M., Hollerbach, J.M. (1988). CONDOR : A Revised Architecture for Controlling Utah/MIT Hand. 1988 IEEE International Conference on Robotics and Automation, pp. 446-449.
- Salisbury, J.K. (1982). Kinematic and Force Analysis of Articulated Hands. Ph.D. Dissertation, Department of Mechanical Engineering, Stanford University, 1982.
- Salisbury, J.K., Craig, J.J. (1982). Articulated Hands : Force Control and Kinematic Issues. International Journal of Robotics Research, vol. 1, no. 1.
- Yoshikawa, T., Nagai, K. (1987). Manipulating and Grasping Forces in Manipulation by Multifingered Hands. 1987 IEEE International Conference on Robotics and Automation, pp. 1998-2004.

